Coefficient Diagram Method Based Decentralized Controller for Fractional Order TITO Systems

Miray Günay Bulut, Furkan Nur Deniz [*]

Abstract— **Fractional calculus has gained increasing attention from researchers because of providing accurate modelling and flexible controller design in control applications. More research to design controllers for Fractional Order Two-Input Two-Output (FOTITO) systems, which inherently have certain difficulties, is needed when the studies on such control applications are reviewed. In this study, Coefficient Diagram Method (CDM) based decentralized controllers are designed for FOTITO systems. To this end, integer order approximate models of FOTITO systems are obtained and decoupled into two subsystems by using simplified and inverted decoupling configurations. The resulting higher-order approximate subsystem transfer functions are reduced by a model reduction method to facilitate CDM-based decentralized controllers design. Then, CDM-based decentralized controllers are designed by using each subsystem, which enable to control the FOTITO system. Simulation results for two different FOTITO systems, one of which is time delayed, show that the proposed approach exhibits successful performance.**

Index Terms— **Coefficient Diagram Method, Decentralized Controller, Fractional Order Systems**

I. INTRODUCTION

INDUSTRIAL SYSTEMS generally consist of multiple-input multiple-output (MIMO) processes which contain multivariable and multiple loops. MIMO systems have complicated loops that cause difficulties on the control of such systems. These complicated loops, where an input variable affects all output variables, can lead to unexpected interaction problems [1].

MİRAY GÜNAY BULUT, is with Department of Electrical and Electronics Engineering University of Adiyaman, Adiyaman, Turkey, (e-mail: mgunay@adiyaman.edu.tr).

https://orcid.org/0000-0001-6479-707X

*FURKAN NUR DENİZ, is with Department of Electrical and Electronics Engineering University of Inonu, Malatya, Turkey, (e-mail: furkan.deniz@inonu.edu.tr).

https://orcid.org/0000-0002-2524-7152

The interaction problems arising in these systems can adversely affect control performance of the system. For this reason, it is necessary to consider the interaction problem when designing controllers for MIMO systems. One of the techniques to eliminate the interaction problem and simplify the controller design is the decoupling technique [2], [3]. Decoupling techniques provide that the MIMO systems are decomposed into single-input single-output (SISO) subsystems by extra decouplers included into the systems, and they enable the design of decentralized controllers for each loop by considering the interaction problems [4]. Various methods such as ideal, simplified and inverted decoupling have been given for the decoupling of systems in the literature [5]–[7]. Among these methods, simplified and inverted decoupling methods are more preferred in applications due to their simplicity [3], [8], [9].

Decoupling methods and formulations are generally applied to two-input two-output (TITO) systems, which are the simplest type of the MIMO systems. Thus, various control strategies developed for TITO systems, which are relatively less complex and easily configurable, can also be generalized for MIMO systems [10]. There are many studies on the design of decentralized controllers for TITO systems using decoupling methods. For example, decentralized controller design based on Characteristic Ratio Assignment (CRA) for TITO systems, which use conventional decoupling method, was presented in [11]. A decentralized PID controller technique was suggested for TITO systems which used reduced models of diagonal elements according to Nyquist plots fitting [12]. An internal model control strategy was proposed for TITO systems by using conventional and inverted decoupling methods [13]. Stability regions of decentralized PI controllers for TITO systems were obtained to calculate all stabilizing controller parameters [8].

Fractional order differential equations more accurately represent the model of a dynamic system [14]. In this direction, various fractional order models have been developed for TITO systems [15]–[17]. Although the fractional order calculus has the advantage of yielding more accurate modeling for dynamic systems, analysis and control of such systems can be quite difficult due to their complexity. Some studies on the fractional order TITO (FOTITO) control systems have been presented in the literature. For example, simplified, inverted and ideal decoupling techniques were expanded for FOTITO systems considering properness and frequency dependent RGA (relative gain array) [16]. An FOTITO model, which has more accurate

time response, for a prototype of a hydraulic canal was proposed by using experimental data [18]. All stabilizing parameters of decentralized PI controllers for an FOTITO thermo-electric temperature process model, which uses inverted and simplified decoupling, were presented [9]. A fractional order IMC (Internal Model Control) methodology, which exhibits robust performance for set point tracking and disturbance rejection, was suggested for FOTITO systems [15]. In another study, fixed low order decentralized controllers were given for FOTITO systems by using optimization according to CRA (Characteristic Ratio Assignment) method [17]. There is a need for more research and development of control algorithms for FOTITO control systems which allow to obtain better and more accurate mathematical models.

In current study, decentralized controllers are designed for FOTITO systems by using the Coefficient Diagram Method (CDM) [19]. Integer order approximate models of FOTITO systems are obtained by using the M-SBL fitting approximation method [20]. Then, the subsystem models, which are configured with simplified and inverted decoupling methods, are used to design decentralized controllers. Since these decoupled approximate models become higher order models, they are transformed to more practicable models suitable for CDM by using a model reduction method [21]. CDM has generally been used to design controllers for SISO systems [19], [22]–[25]. Since industrial systems consist of MIMO systems, CDM based controller design has been extended to MIMO systems. In one of Manabe's studies on MIMO systems [26], CDM was used to control a dual-control surface missile. In the same study, Manabe additionally decomposed MIMO systems into single-input multiple-output (SIMO) systems and performed controller design by applying the CDM design procedure to each SIMO system. Similarly, in another study [27], Manabe applied the CDM in the control of a fighter with dual control surfaces, which consists of a MIMO system. Also, decentralized controller design [28], decentralized PI controller [29], [30] and PID controller [31] designs by using CDM were presented for TITO systems. In this study, unlike the others, the systems are fractional order systems which bring design difficulties due to its nature.

The main advantage of CDM is the ability to predefine specifications of time response such as settling time and overshoot during the design process [25]. Thus, CDM offers the possibility to guarantee a simple and robust controller design [25]. The basic properties of CDM are briefly as follows; i) There is a little or no overshoot. ii) Two degrees of freedom (2DOF) control system is used. iii) It has robust performance to changes in parameters and limited uncertainties in the control system. iv) It provides convenience to the designer thanks to the predefined settling time [22]–[25]. In this study, CDM based decentralized controllers are designed for two different FOTITO systems, and simulation results validate that the proposed approach provides good performance.

II. FRACTIONAL ORDER TITO SYSTEMS AND DECOUPLING METHODS

A FOTITO system can be expressed as a transfer function matrix given below.

$$G(s) = \begin{bmatrix} G_{11}(s) & G_{12}(s) \\ G_{21}(s) & G_{22}(s) \end{bmatrix} \qquad (1)$$

where each element of transfer function matrix $G_{ij}(s) = \sum_{m=0}^{p} u_m s^{\beta_m} / \sum_{n=0}^{q} v_n s^{\alpha_n}$ can be expressed as fractional-order transfer functions for $\alpha_i, \beta_j \in R$, $i, j = 1, 2$. $G_{ij}(s) = K_{ij} e^{-\theta_{ij} s} / (T_{ij} s^{\alpha_{ij}} + 1)$ can be expressed as a fractional order system with time delay. The time delay should be considered while applying the decoupling techniques to FOTITO systems. In this context, if $\theta_{11} \le \theta_{12}$ and $\theta_{22} \le \theta_{21}$, the decoupler becomes causal and can be realized easily [32].

When the system is an FOTITO process, decoupling methods can be applied to facilitate the design of the controllers by considering the interaction problem [16]. The most well-known decoupling methods are ideal, simplified and inverted decoupling methods [33]. Researchers should decide on the selection of the decoupling method for the system by considering the advantages and disadvantages of these methods. The advantage of ideal decoupling is that the controller transfer matrix is very easy to determine, the disadvantage is that it has realization problems due to the complexity of the decoupler elements [34]. In simplified decoupling, the values of the diagonal elements of the decoupler matrix are assumed to be 1, so it is easy to determine the decoupling elements. Weischedel et al. [6] observed that simplified decoupling is more robust compared to ideal decoupling in their study. The inverted decoupling has a combination of the positive properties of ideal and simplified decouplings [7]. In this study, the simplified and inverted decoupling methods are applied to FOTITO systems. Fig. 1 shows the block diagrams of simplified and inverted decoupling methods.

The decoupling transfer function matrix $D(s)$ and the diagonal transfer function matrix $T(s)$ can be written as follows [33],

$$D(s) = \begin{bmatrix} D_{11}(s) & D_{12}(s) \\ D_{21}(s) & D_{22}(s) \end{bmatrix} \qquad (2)$$

$$T(s) = \begin{bmatrix} T_1(s) & 0 \\ 0 & T_2(s) \end{bmatrix} = G(s) D(s) \qquad (3)$$

The decoupler transfer function matrix of the simplified and inverted decouplings are the same and expressed as follows:

$$D(s) = G(s)^{-1} T(s) = \begin{bmatrix} 1 & -\dfrac{G_{12}(s)}{G_{11}(s)} \\ -\dfrac{G_{21}(s)}{G_{22}(s)} & 1 \end{bmatrix} \qquad (4)$$

       http://dergipark.gov.tr/bajece

The diagonal transfer matrix $T(s)$ of the simplified decoupling is calculated by using Equations (1), (3) and (4) as follows:

$$T(s) = \begin{bmatrix} G_{11}(s) - \dfrac{G_{12}(s)G_{21}(s)}{G_{22}(s)} & 0 \\ 0 & G_{22}(s) - \dfrac{G_{12}(s)G_{21}(s)}{G_{11}(s)} \end{bmatrix} \quad (5)$$

The diagonal transfer matrix $T(s)$ of the inverted decoupling is calculated as:

$$T(s) = \begin{bmatrix} T_1(s) & 0 \\ 0 & T_2(s) \end{bmatrix} = \begin{bmatrix} G_{11}(s) & 0 \\ 0 & G_{22}(s) \end{bmatrix} \quad (6)$$

The diagonal transfer matrix of the controller $C(s)$ is defined as

$$C(s) = \begin{bmatrix} C_1(s) & 0 \\ 0 & C_2(s) \end{bmatrix} \quad (7)$$
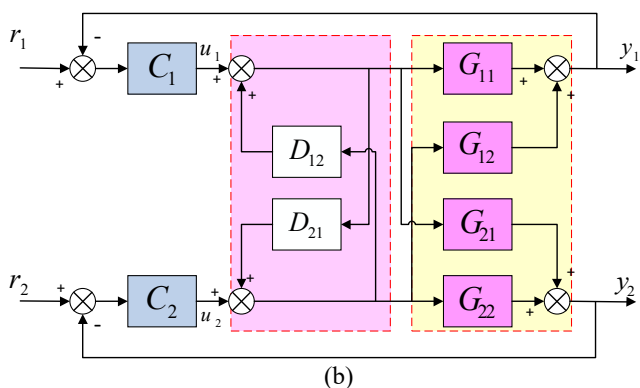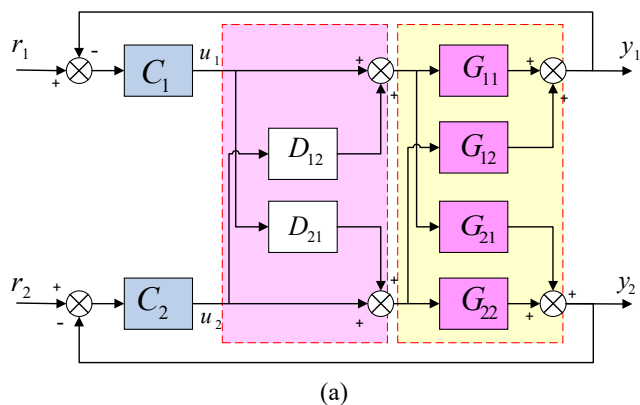

(a)

(b)

Fig.1. a) Simplified decoupling, b) Inverted decoupling

FOTITO system is decoupled into two SISO subsystems by using simplified and inverted decoupling, and the transfer function of each subsystem is denoted as $T_i(s)$, and its controller is denoted as $C_i(s)$ for $(i=1,2)$.
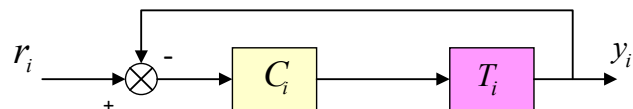
Block diagram of each subsystem is given in Figure 2.

Fig.2. Feedback control system for subsystems.

III. COEFFICIENT DIAGRAM METHOD

Coefficient Diagram Method developed by Manabe in 1991 [19], is an algebraic method that is used to design a high order controller. CDM is a polynomial approach where the numerator and denominator polynomials of the transfer function of the system are treated independently. The advantage of the CDM based control system is to predefine settling time and maximum overshoot at the beginning of the design task [25].

CDM based configuration illustrated in Fig. 3 has a two-degree of freedom control system, which can better perform in respect to set-point tracking and disturbance rejection [35].
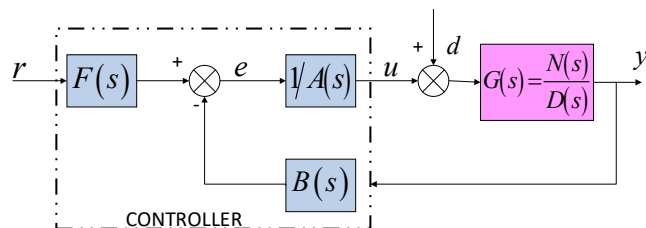

Fig.3. CDM based control system

In the CDM based control system in Fig. 3, $N(s)$ and $D(s)$ are numerator and denominator polynomials of the plant transfer function $G(s)$, respectively. $A(s)$ is denominator of the controller, $B(s)$ is feedback numerator of the controller, and $F(s)$ is the reference numerator of the controller [19].

The output of this control system can be written as follows [25].

$$y = \frac{N(s)F(s)}{P(s)} r + \frac{A(s)N(s)}{P(s)} d \quad (8)$$

Characteristic polynomial of the closed loop system is

$$P(s) = D(s)A(s) + N(s)B(s) = \sum_{i=0}^{n} a_i s^i \quad (9)$$

where the controller polynomials $A(s)$ and $B(s)$ are defined as

$$A(s) = \sum_{i=0}^{p} l_i s^i \text{ and } B(s) = \sum_{i=0}^{q} k_i s^i \text{ ; } p \ge q \quad (10)$$

Reference numerator of the controller $F(s)$ is

$$F(s) = (P(s)/N(s))_{s=0} \quad (11)$$

There is an important point to be considered in the selection of $A(s)$ and $B(s)$ polynomials. In order to achieve the desired time response performance, if the system transfer function does not include an integrator, $l_0 = 0$ should be selected to completely eliminate the effects of the disturbance [28].

CDM design parameters are expressed with equivalent time constant τ, stability index γ_i and stability limit index γ_i^* [19]. They can be written in terms of the coefficients of the characteristic polynomial as follows:

$$\tau = \frac{a_1}{a_0}, \quad \gamma_i = \frac{a_i^2}{(a_{i-1} a_{i+1})}; i = 1,....,n-1$$

$$\gamma_i^* = \frac{1}{\gamma_{i+1}} + \frac{1}{\gamma_{i-1}}; \gamma_0 = \gamma_n = \infty \tag{12}$$

Manabe proposed that the stability indexes are selected as $\gamma_1 = 2.5$, $\gamma_i = 2$ and $\gamma_0 = \gamma_n = \infty$ for $i = 2 \sim (n-1)$ so that CDM based controller design provides the desired performance [19]. These proposed values can be changed to achieve the desired control performance according to $\gamma_i > 1.5$ for all $i = 1 \sim (n-1)$ [28]. Using these parameters, the coefficients of the characteristic polynomial are determined as follows:

$$a_i = \frac{a_0 \tau^i}{\gamma_{i-1} \gamma_{i-2}^2 ......\gamma_1^{i-1}} \tag{13}$$

According to the standard Manabe form [19], the settling time is calculated with $\tau = t_s / (2.5 \sim 3)$. After determining the desired settling time and stability indexes of the system, the target characteristic polynomial is defined with the equation given below [28].

$$P_{\text{target}}(s) = a_0 \left[\left\{ \sum_{i=2}^{n} \left(\prod_{j=1}^{i-1} \frac{1}{\gamma_{i-j}^j} \right) (\tau s)^i \right\} + \tau s + 1 \right] \tag{14}$$

By matching the target characteristic polynomial to the characteristic polynomial of the system, the controller parameters k_i and l_i can be calculated as follows.

$$A(s) D(s) + B(s) N(s) = P_{\text{target}}(s) \tag{15}$$

When the CDM based control system is adapted to the 2DOF control system as given in Fig. 4, it exhibits better performance for set point tracking and disturbance rejection [22]
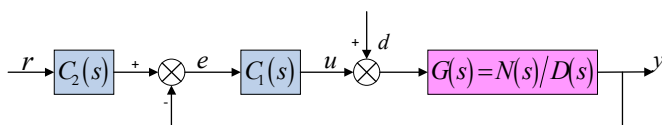

Fig. 4. Two-degree-of-freedom (2DOF) control system

The controllers $C_1(s)$ and $C_2(s)$ are defined by using the CDM polynomials as follows:

$$C_1(s) = \frac{B(s)}{A(s)}, \; C_2(s) = \frac{F(s)}{B(s)} \tag{16}$$

This modification, which is made according to the 2DOF control system, facilitates the use of CDM in FOTITO systems with decoupling. The simplified and inverted decoupling block diagrams can be redesigned by using the 2DOF structure [31] as shown in Fig. 5, respectively. In Equation (16), $C_{11}(s)$ and $C_{12}(s)$ correspond to $C_1(s)$ and $C_2(s)$ for r₁-y₁ relation and $C_{21}(s)$ and $C_{22}(s)$ correspond to $C_1(s)$ and $C_2(s)$ r₂-y₂ relation, respectively.
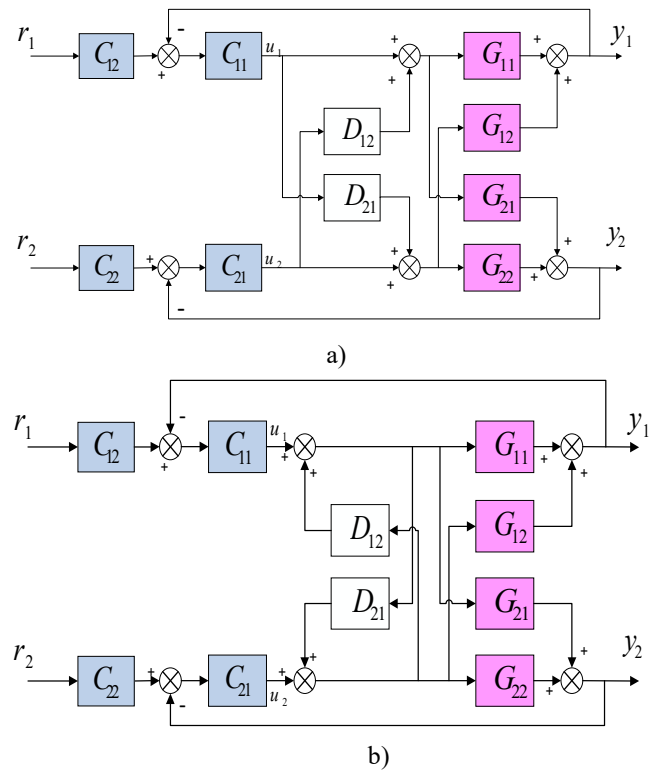

a)

b)

Fig. 5. Modified FOTITO systems based on 2DOF control: a) simplified decoupling b) inverted decoupling.

IV. APPROXIMATE MODELS FOR IMPLEMENTING FRACTIONAL ORDER TRANSFER FUNCTIONS

The realization of fractional order derivative and integrator operators is inherently difficult due to their long memory effects [36]. Therefore, approximate integer order models of fractional order operators are used in the realization task. Several approximation methods such as Oustaloup's method [37], Matsuda's method [38], SBL (Stability Boundary Locus) fitting method [39] and its modified version M-SBL (Modified Stability Boundary Locus) fitting method [20] were presented in the literature to obtain these approximate models. In this study,

authors prefer to use the M-SBL fitting approximation method [20], which is based on fitting the stability boundary curves of the fractional order operator with its integer order approximation model. Thus, it can be ensured that the integer order approximate models can preserve stabilization of fractional order transfer functions in the realization process [40].

Using M-SBL fitting approximation method, one can obtain an nth integer order approximate model for a fractional order derivative operator s^α in a desired frequency range $\omega \in [\omega_l, \omega_h]$ rad/sec as follows:

$$s^\alpha = \frac{a_0 s^n + a_1 s^{n-1} + \dots\dots + a_{n-1} s + a_n s^0}{a_n s^n + a_{n-1} s^{n-1} + \dots\dots + a_1 s + a_0 s^0} , \ 0 < \alpha < 1 \qquad (17)$$

The M-SBL fitting Matlab function [41] is used to obtain the integer order approximate transfer functions of the fractional order derivative operators. This subject was studied in [20] comprehensively.

V. SUB-OPTIMAL MODEL REDUCTION

The sub-optimal model reduction is a reduction method based on optimization, and its algorithms are simple [21]. This method reduces the size of the coefficient matrix of the system while preserving the dominant eigenvalues or most important states of the original system. Target of the model reduction method is that it can easily reduce the model to the most realistic and desired degree [21].

ISE (Integral Square Error) criterion commonly used in determining the quality of the reduced model according to the error signal $e(t)$ is expressed as follows.

$$I_{ISE} = \int_0^\infty e^2(t) dt \qquad (18)$$

Using the ISE criterion, the error rate is minimized, and the model reduction problem is converted into an optimization problem. The approximate error of the model can be written as $\hat{e}(t, \theta)$ for a particular original model and input signal. The sub-optimal model reduction objective function can be given as follows:

$$J = \min_\theta \left[\int_0^\infty \omega^2(t) \hat{e}^2(t, \theta) dt \right] \qquad (19)$$

where $\omega(t)$ is the weighting function, $\theta = [\alpha_1, \dots, \alpha_k, \beta_1, \dots, \beta_{r+1}, \tau]^T$ is the parameter vector. In this study, the sub-optimal Matlab function algorithm given in [21] is used to reduce the high order transfer functions to the models of desired orders.

VI. SIMULATION RESULTS

In this section, two examples are given to demonstrate the decentralized controller design by using the coefficient diagram method for FOTITO systems. At first, the integer order approximate models of the FOTITO systems are obtained by using the M-SBL fitting approximation method. Then, the FOTITO systems are decoupled into two subsystems by appropriate decoupling methods. The integer order approximate models are remarkably high order models and not suitable for CDM based decentralized controller design. For this reason, the approximate models are brought into suitable forms for the design by using the mentioned model reduction method. Finally, the CDM based decentralized controller design procedure is applied.

Example 1: Let us consider an FOTITO system [17] which has the transfer function matrix

$$G(s) = \begin{bmatrix} \dfrac{1}{2s^{1.4} + s^{0.7} + 1} & \dfrac{1}{s^{1.4} + 0.5s^{0.7} + 0.5} \\ \dfrac{0.5}{0.5s^{1.4} + 0.5s^{0.7} + 0.4} & \dfrac{1}{0.5s^{1.4} + s^{0.7} + 1.2} \end{bmatrix} \qquad (20)$$

M-SBL fitting approximation method is applied to obtain 4th integer order approximate models of fractional order operators s^α in the frequency range $\omega \in [10^{-1}, 10^1]$ rad/sec, and by using this approximate models, integer order approximate transfer functions of FOTITO systems are calculated as high order transfer functions. Details are given in appendix.

High order transfer functions complicate the design of the CDM based decentralized controller. Therefore, using the sub-optimal model reduction method [21], the reduced transfer function matrix elements are obtained as follows.

$$G_{r11}(s) = \frac{0.2136s^2 + 0.5841s + 0.06934}{s^3 + 1.584s^2 + 0.7807s + 0.07191} \qquad (21)$$

$$G_{r12}(s) = \frac{0.4273s^2 + 1.168s + 0.1387}{s^3 + 1.584s^2 + 0.7806s + 0.07191} \qquad (22)$$

$$G_{r21}(s) = \frac{0.2059s^2 + 2.764s + 0.3635}{s^3 + 4.879s^2 + 3.162s + 0.3043} \qquad (23)$$

$$G_{r22}(s) = \frac{0.1995s^2 + 15.54s + 2.569}{s^3 + 20.35s^2 + 24.9s + 3.178} \qquad (24)$$

Fig. 6 shows that step responses of the fractional order transfer matrix elements in Equation (20), their integer order approximate transfer functions and their reduced transfer functions match successfully. Step responses of the fractional order transfer functions are obtained by using fotf function in [21]. Considering the matching of the unit step responses, the 2nd degree numerator and the 3rd degree denominator polynomials were used.
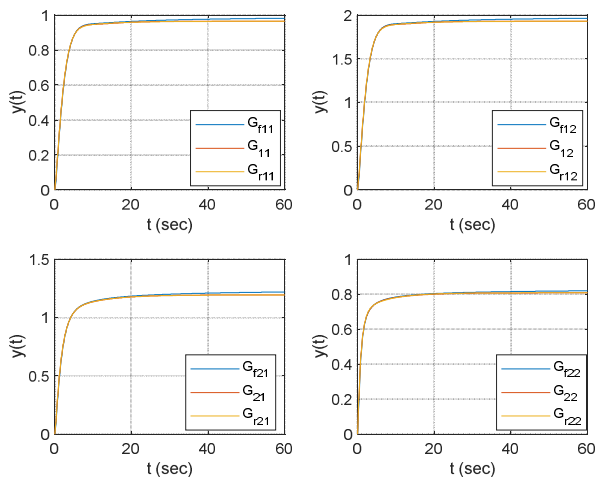
Fig. 6. The step responses of the fractional order transfer matrix elements $G_{fij}(s)$, their integer order approximate transfer functions $G_{ij}(s)$, and their reduced transfer functions $G_{rij}(s)$.

In this example, the system is decoupled with simplified decoupling to eliminate the interaction. Thus, the decoupler matrix elements of simplified decoupling, which are calculated with equation (4) by using the reduced transfer functions, are obtained as follows:

$$D_{r12}(s) = \frac{-G_{r12}(s)}{G_{r11}(s)} = \frac{\begin{array}{c}-0.4273s^5 - 1.845s^4 - 2.323s^3\\ -1.162s^2 - 0.1923s - 0.009972\end{array}}{\begin{array}{c}0.2136s^5 + 0.9225s^4 + 1.161s^3\\ +0.5811s^2 + 0.09613s + 0.004986\end{array}} \quad (25)$$

$$D_{r21}(s) = \frac{-G_{r21}(s)}{G_{r22}(s)} = \frac{\begin{array}{c}-0.2059s^5 - 6.955s^4 - 61.74s^3\\ -76.87s^2 - 17.83s - 1.155\end{array}}{\begin{array}{c}0.1995s^5 + 16.51s^4 + 79.01s^3\\ +61.72s^2 + 12.85s + 0.7818\end{array}} \quad (26)$$

The diagonal transfer matrix elements are calculated by using the approximate transfer functions of the FOTITO system in Equation (20). Since the obtained transfer functions are remarkably high order, the diagonal transfer matrix elements are redefined as follows using model reduction.

$$T_{r1}(s) = \frac{N_{r1}(s)}{D_{r1}(s)} = \frac{0.03348s^2 - 0.557s - 0.09187}{s^3 + 1.126s^2 + 0.4854s + 0.04872} \quad (27)$$

$$T_{r2}(s) = \frac{N_{r2}(s)}{D_{r2}(s)} = \frac{0.01349s^2 - 1.522s - 0.2131}{s^3 + 2.466s^2 + 1.405s + 0.1348} \quad (28)$$

After the suitable transfer functions are defined, the task of designing a CDM based decentralized controller can be performed. The numerator and denominator polynomials of the transfer functions $T_{r1}(s)$ and $T_{r2}(s)$ are given in the above equations.

According to Equation (10), polynomials $A(s)$ and $B(s)$ can be defined as follows.

$$A(s) = l_3 s^3 + l_2 s^2 + l_1 s + l_0 \quad (29)$$

$$B(s) = k_3 s^3 + k_2 s^2 + k_1 s + k_0 \quad (30)$$

where $l_0 = 0$ is used to provide the disturbance rejection on the system [28].
The characteristic polynomial of the CDM control system, which consists of decentralized controller parameters and the subsystem transfer function $T_{r1}(s)$, can be written as

$$\begin{array}{l}P(s) = \left(l_3 s^3 + l_2 s^2 + l_1 s^1\right)\left(s^3 + 1.126s^2 + 0.4854s + 0.04872\right)\\ + \left(k_3 s^3 + k_2 s^2 + k_1 s^1 + k_0\right)\left(0.03348s^2 - 0.557s - 0.09187\right)\end{array} \quad (31)$$

The target characteristic polynomial, which is determined with CDM parameters $\tau = 10$, $\gamma_1 = 3.4$, $\gamma_2 = 2$ $\gamma_3 = 2$, $\gamma_4 = 2$, $\gamma_5 = 2$, is obtained as

$$\begin{array}{l}P_{\text{target}}(s) = 2.149s^6 + 11.69s^5 + 31.8s^4\\ + 43.25s^3 + 29.41s^2 + 10s + 1\end{array} \quad (32)$$

By matching Equation (31) and Equation (32), the polynomials of the decentralized controller are obtained as follows:

$$A(s) = 2.1490s^3 + 11.6124s^2 - 18.0864s \quad (33)$$

$$B(s) = -69.9564s^3 - 95.5171s^2 - 52.4465s - 10.8849 \quad (34)$$

In addition, $F(s) = -10.8849$ can be calculated by using Equation (11). The decentralized controllers $C_{11}(s)$ and $C_{12}(s)$ given in Fig. 5a are obtained as follows:

$$C_{11}(s) = \frac{-69.9564s^3 - 95.5171s^2 - 52.4465s - 10.8849}{2.1490s^3 + 11.6124s^2 - 18.0864s} \quad (35)$$

$$C_{12}(s) = \frac{-10.8849}{-69.9564s^3 - 95.5171s^2 - 52.4465s - 10.8849} \quad (36)$$

The characteristic polynomial for the CDM control system using the subsystem $T_{r2}(s)$ is calculated as follows:

$$\begin{array}{l}P(s) = \left(l_3 s^3 + l_2 s^2 + l_1 s^1\right)\left(s^3 + 2.466s^2 + 1.405s + 0.1348\right)\\ + \left(k_3 s^3 + k_2 s^2 + k_1 s^1 + k_0\right)\left(0.01349s^2 - 1.522s - 0.2131\right)\end{array} \quad (37)$$

Substituting the $\tau = 10$, $\gamma_1 = 4.5$, $\gamma_2 = 2.2$, $\gamma_3 = 2$, $\gamma_4 = 2$, $\gamma_5 = 2$ parameters in Equation (14), the target characteristic polynomial is obtained as follows:

$$\begin{array}{l}P_{\text{target}}(s) = 0.3615s^6 + 2.863s^5 + 11.34s^4\\ + 22.45s^3 + 22.22s^2 + 10s + 1\end{array} \quad (38)$$

Polynomials of the decentralized controller $A(s) = 0.3615s^3 + 2.1044s^2 - 9.0065s$, $F(s) = -4.6926$ and

$$B(s) = -9.8547s^3 - 26.1558s^2 - 19.1079s - 4.6926$$

are computed for $T_{r2}(s)$ by using Equation (37) and Equation (38).

The decentralized controllers $C_{21}(s)$ and $C_{22}(s)$ given in Fig. 5a are obtained as follows:

$$C_{21}(s) = \frac{-9.8714s^3 - 26.1920s^2 - 19.1222s - 4.6926}{0.3615s^3 + 2.1047s^2 - 9.0291s} \quad (39)$$

$$C_{22}(s) = \frac{-4.6926}{-9.8714s^3 - 26.1920s^2 - 19.1222s - 4.6926} \quad (40)$$

A unit step function with an amplitude of 0.1 at $t = 50$ sec is given to the FOTITO system as a disturbance signal. When the FOTITO system is performed with CDM based decentralized controllers, the unit step responses are obtained as given in Fig. 7.
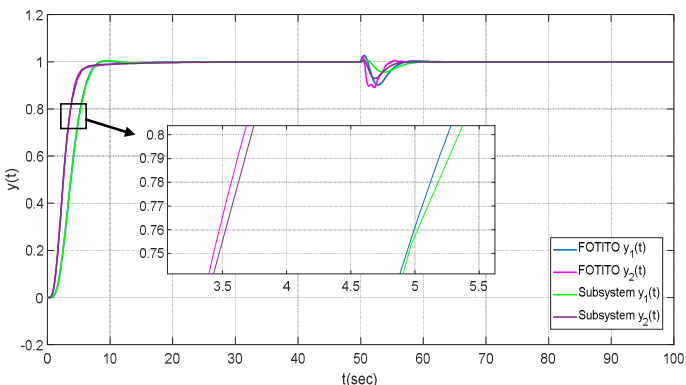

Fig. 7. The step responses of the FOTITO system with simplified decoupling

The unit step responses obtained for the subsystems $T_{r1}(s)$, $T_{r2}(s)$ and the FOTITO system are shown in Fig. 7. It can be seen from this figure that the CDM-based decentralized controllers obtained for the subsystems provide successful performance when placed in the FOTITO system using simplified decoupling.
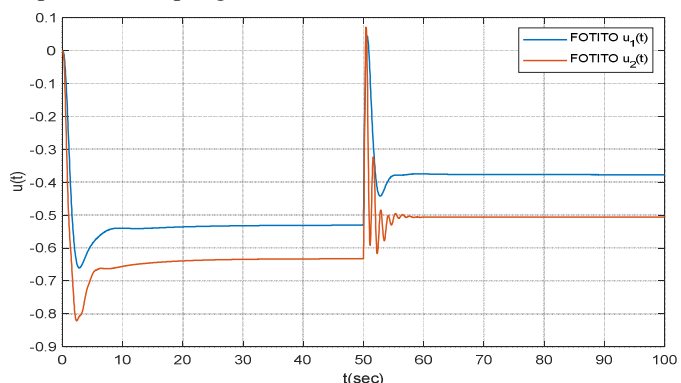

Fig 8. Control signals generated by the FOTITO system with simplified decoupling

The control signals generated by the decentralized controllers in the FOTITO system are given in Fig.8. Although the previous studies that controllers can be unstable in control systems with

CDM [22], the control signals of the FOTITO system are acceptable in terms of saturation limits.

The performance values of the step responses shown in Fig. 7 are listed in Table I. As seen in Table I and Fig. 7, the system controlled by the CDM based decentralized controllers exhibits a successful control performance in respect to the settling time and maximum overshoot. In addition, when a disturbance signal is applied to the system, the CDM based decentralized controllers provide satisfactory disturbance rejection.

TABLE I
PERFORMANCE VALUES OF THE STEP RESPONSES IN FIG. 7

PERFORMANCE VALUES	FOTITO y_1	FOTITO y_2	Subsystem y_1	Subsystem y_2
Settling Time	7.4843	7.0743	7.6272	6.3575
Maximum Overshoot (%)	0.3338	0	0.5021	0.0180

In this example, the stability index and equivalent time constant values, which are different from the values proposed by Manabe, are used to achieve better time response performance. Settling time and maximum overshoot are obtained as given in the Table I according to the selected values. Depending on the selected values, it can be seen that the ratio between t_s and τ suggested by Manabe [19] is relatively smaller. One can say that better results can be obtained depending on the selected stability index values and equivalent time constant.

Example 2: Consider the following FOTITO system with time delay as given in [15],

$$G(s) = \begin{bmatrix} \dfrac{1.2e^{-0.2s}}{2s^{0.5}+1} & \dfrac{0.6e^{-0.3s}}{3s^{0.7}+1} \\ \dfrac{0.5e^{-0.4s}}{s^{0.8}+1} & \dfrac{1.5e^{-0.3s}}{3s^{0.6}+1} \end{bmatrix} \quad (41)$$

Similar to the example 1, 4th integer order approximate models of fractional order operators s^{α} in the frequency range $\omega \in [10^{-1}, 10^{1}]$ rad/sec are obtained by using the M-SBL fitting approximation method. Then, the integer order approximate transfer functions of the FOTITO system are calculated by using the obtained 4th order approximate models (in appendix), and 1st order Pade approximation [22] is used for time delay elements.

The following reduced transfer functions are obtained by applying the sub-optimal model reduction method [21] to integer order approximate transfer functions to facilitate controller design with CDM.

$$G_{r11}(s) = \frac{117.2s + 16.57}{s^4 + 4.879s^3 + 180.9s^2 + 209.1s + 16.89} \quad (42)$$

$$G_{r12}(s) = \frac{8.648s + 1.36}{s^4 + 4.155s^3 + 50.41s^2 + 31.25s + 2.519} \quad (43)$$

$$G_{r21}(s) = \frac{10.61s + 2.009}{s^4 + 5.885s^3 + 31.61s^2 + 29.91s + 4.092} \quad (44)$$

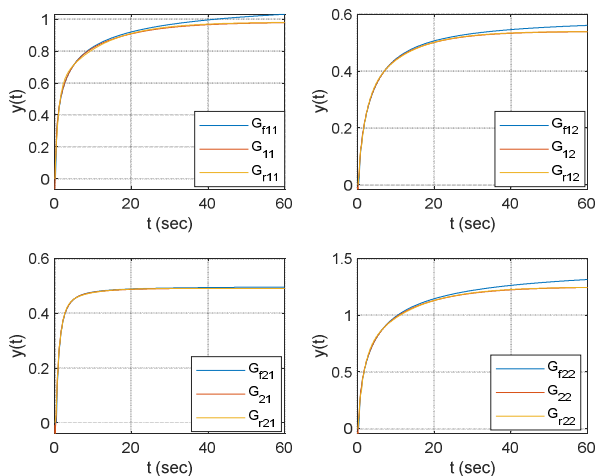$$G_{r22}(s) = \frac{28.6s + 4.112}{s^4 + 3.859s^3 + 63.93s^2 + 45.47s + 3.289} \quad (45)$$

Fig. 9. The step responses of the fractional order transfer matrix elements $G_{fij}(s)$, their integer order approximate transfer functions $G_{ij}(s)$, and their reduced transfer functions $G_{rij}(s)$.

Fig. 9 shows step responses of the fractional order transfer matrix elements in Equation (41), their integer order approximate transfer functions and their reduced transfer functions. One can say that the step responses match satisfactorily.

In this example, the system is decoupled with inverted decoupling method. When reduced transfer functions are substituted in Equation (4), decoupler transfer function matrix elements are calculated as follows.

$$D_{r12}(s) = \frac{\begin{array}{c} -8.648s^5 - 43.56s^4 - 1571s^3 \\ -2055s^2 - 430.4s - 22.97 \end{array}}{\begin{array}{c} 117.2s^5 + 503.6s^4 + 5977s^3 \\ +4497s^2 + 813s + 41.74 \end{array}} \quad (46)$$

$$D_{r21}(s) = \frac{\begin{array}{c} -10.61s^5 - 42.96s^4 - 686.2s^3 \\ -611s^2 - 126.3s - 6.608 \end{array}}{\begin{array}{c} 28.6s^5 + 172.5s^4 + 928.3s^3 \\ +985.4s^2 + 240s + 16.83 \end{array}} \quad (47)$$

The subsystem transfer functions of the FOTITO system given in Equation (41) are obtained as follows for the inverted decoupling.

$$T_{r11}(s) = \frac{117.2s + 16.57}{s^4 + 4.879s^3 + 180.9s^2 + 209.1s + 16.89} \quad (48)$$

$$T_{r22}(s) = \frac{28.6s + 4.112}{s^4 + 3.859s^3 + 63.93s^2 + 45.47s + 3.289} \quad (49)$$

Since both $T_{r1}(s)$ and $T_{r2}(s)$ subsystems are 4th order, polynomials $A(s)$ and $B(s)$ are expressed as follows.

$$A(s) = l_4s^4 + l_3s^3 + l_2s^2 + l_1s \quad (50)$$

$$B(s) = k_4s^4 + k_3s^3 + k_2s^2 + k_1s + k_0 \quad (51)$$

CDM based decentralized controller design is applied by selecting parameters $\tau = 10$, $\gamma_1 = 6$, $\gamma_2 = 5$, $\gamma_3 = 2$, $\gamma_4 = 2$, $\gamma_5 = 2$, $\gamma_6 = 2$ and $\gamma_7 = 2$ for $T_{r1}(s)$ and $T_{r2}(s)$ transfer functions.

The parameters determined in the CDM based decentralized controller design are selected the same for both transfer functions, so their target characteristic polynomials are also the same:

$$\begin{aligned} P_{\text{target}}(s) = {} & 6.977e - 07s^8 + 6.698e - 05s^7 + 0.003215s^6 \\ & + 0.07716s^5 + 0.9259s^4 + 5.556s^3 + 16.67s^2 + 10s + 1 \end{aligned} \quad (52)$$

Characteristic polynomial for $T_{r1}(s)$ is obtained by substituting the determined parameters in Equation (9) as follows.

$$\begin{aligned} P_1(s) = {} & \left(l_4s^4 + l_3s^3 + l_2s^2 + l_1s^1\right)\binom{s^4 + 4.879s^3 + 180.9s^2}{+209.1s + 16.89} \\ & + \left(k_4s^4 + k_3s^3 + k_2s^2 + k_1s^1 + k_0\right)(117.2s + 16.57) \end{aligned} \quad (53)$$

$A(s)$, $B(s)$ and $F(s)$ are obtained by matching the target characteristic polynomial to the characteristic polynomial of the transfer function $T_{r1}(s)$.

$$A(s) = 0.00001s^4 + 0.0001s^3 + 0.0028s^2 - 0.0744s \quad (54)$$

$$\begin{aligned} B(s) = {} & 0.0011s^4 + 0.0064s^3 + 0.1564s^2 \\ & + 0.2525s + 0.0604 \end{aligned} \quad (55)$$

$$F(s) = 0.0604 \quad (56)$$

The characteristic polynomial for CDM control system using $T_{r2}(s)$ is

$$\begin{aligned} P_2(s) = {} & \left(l_4s^4 + l_3s^3 + l_2s^2 + l_1s^1\right)\binom{s^4 + 3.859s^3 + 63.93s^2}{+45.47s + 3.289} \\ & + \left(k_4s^4 + k_3s^3 + k_2s^2 + k_1s^1 + k_0\right)(28.6s + 4.112) \end{aligned} \quad (57)$$

By matching Equation (52) with Equation (57), $A(s)$, $B(s)$ and $F(s)$ for $T_{r2}(s)$ transfer function are obtained as follows:

$$A(s) = 0.00001s^4 + 0.0001s^3 + 0.0029s^2 - 0.3918s \quad (58)$$

$$B(s) = 0.0159s^4 + 0.0763s^3 + 1.0544s^2 \\ + 1.0538s + 0.2432 \quad (59)$$

$$F(s) = 0.2432 \quad (60)$$

CDM based decentralized controllers shown in Fig. 5b are obtained according to the given parameters as follows:

$$C_{11}(s) = \frac{0.0011s^4 + 0.0064s^3 + 0.1564 + 0.2525s + 0.0604}{0.000001s^4 + 0.0001s^3 + 0.0028s^2 - 0.0744s} \quad (61)$$

$$C_{12}(s) = \frac{0.0604}{0.0011s^4 + 0.0064s^3 + 0.1564 + 0.2525s + 0.0604} \quad (62)$$

$$C_{21}(s) = \frac{0.0159s^4 + 0.0763s^3 + 1.0544s^2 + 1.0538s + 0.2432}{0.000001s^4 + 0.0001s^3 + 0.0029s^2 - 0.3918} \quad (63)$$

$$C_{22}(s) = \frac{0.2432}{0.0159s^4 + 0.0763s^3 + 1.0544s^2 + 1.0538s + 0.2432} \quad (64)$$

A unit step function with an amplitude of 0.1 at $t = 30$ sec is given to the system shown in Fig. 5b as a disturbance signal. When the system given in Fig. 5b is simulated for the obtained CDM based decentralized controllers, the unit step responses and the control signals given in Fig. 10 and Fig. 11 are obtained.
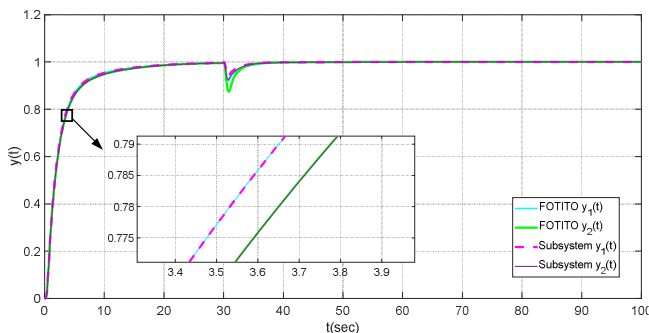

Fig. 10. The step responses of the FOTITO system with inverted decoupling.

Fig. 10 demonstrates that the CDM-based decentralized controllers obtained for subsystems exhibit good performance when placed in the FOTITO system using inverted decoupling. Similar to the example 1, one can say that the amplitudes of the control signals in Figure 11 do not affect the saturation negatively.

Performance values of the unit step responses shown in Fig. 10 are listed in Table II. The values in Table II validate that the maximum overshoot does not occur when the proposed the CDM-based decentralized controllers are used in the FOTITO system. As in the first example, the settling time is different because the equivalent time constant and stability index were selected different from those suggested by Manabe.
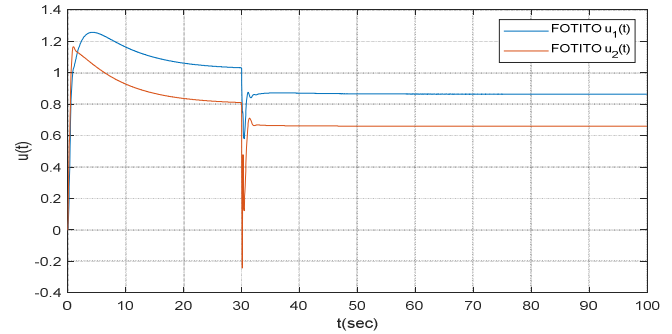

Fig 11. Control signals generated by the FOTITO system with inverted decoupling

TABLE II
PERFORMANCE VALUES OF THE STEP RESPONSES IN FIG. 10

PERFORMANCE VALUES	FOTITO y_1	FOTITO y_2	Subsystem y_1	Subsystem y_2
Settling Time	16.2669	17.2318	16.1515	17.0949
Maximum Overshoot (%)	0	0	0	0

VII. CONCLUSIONS

In this study, CDM based decentralized controllers are designed for FOTITO systems. Integer order approximate models of FOTITO systems are obtained by using the M-SBL fitting approximation method. These approximate models are decoupled into two subsystems using simplified and inverted decoupling methods. The transfer functions of the decoupled subsystems are obtained as high order. CDM-based decentralized controller design is difficult for the high-order subsystem transfer functions. Therefore, the orders of subsystem transfer functions are reduced by using the model reduction algorithm in order to facilitate the design of decentralized controller with CDM. The decentralized controllers are designed by using CDM for the transfer functions of reduced subsystems. Satisfactory results are obtained by placing the decentralized controllers, which are calculated for the subsystems, in the FOTITO systems configuration. In other words, it is concluded that CDM based decentralized controllers, which are designed for subsystems obtained by simplified and inverted decouplings, provide successful performance for FOTITO systems.

Appendix:

Integer order approximate transfer functions of the FOTITO system in Example 1 are

$$G_{11}(s) = \frac{\begin{array}{c} s^8 + 99.68s^7 + 2632s^6 + 1.873e04s^5 + 5.04e04s^4 + 5.205e04s^3 \\ + 2.174e04s^2 + 3205 + 149.9 \end{array}}{\begin{array}{c} 11.13s^9 + 909.1s^8 + 1.416e04s^7 + 7.667e04s^6 + 1.737e05s^5 \\ + 1.898e05s^4 + 1.064e05s^3 + 3.046e04s^2 + 3700s + 155.5 \end{array}}$$

$$G_{12}(s) = \frac{\begin{matrix} s^8 + 99.68s^7 + 2632s^6 + 1.873e04s^5 + 5.04e04s^4 + 5.205e04s^3 \\ + 2.174e04s^2 + 3205s + 149.9 \end{matrix}}{\begin{matrix} 5.567s^9 + 454.6s^8 + 7081s^7 + 3.833e04s^6 + 8.687e04s^5 \\ + 9.491e04s^4 + 5.32e04s^3 + 1.523e04s^2 + 1850s + 77.74 \end{matrix}}$$

$$G_{21}(s) = \frac{\begin{matrix} 0.5s^8 + 49.84s^7 + 1316s^6 + 9363s^5 + 2.52e04s^4 + 2.602e04s^3 \\ + 1.087e04s^2 + 1603s + 74.95 \end{matrix}}{\begin{matrix} 2.784s^9 + 234.2s^8 + 3837s^7 + 2.245e04s^6 + 5.656e04s^5 \\ + 6.923e04s^4 + 4.222e04s^3 + 1.249e04s^2 + 1516s + 62.74 \end{matrix}}$$

$$G_{22}(s) = \frac{\begin{matrix} s^8 + 99.68s^7 + 2632s^6 + 1.873e04s^5 + 5.04e04s^4 + 5.205e04s^3 \\ + 2.174e04s^2 + 3205 + 149.9 \end{matrix}}{\begin{matrix} 2.784s^9 + 248.4s^8 + 4482s^7 + 3.034e04s^6 + 9.218e04s^5 \\ + 1.38e05s^4 + 9.948e04s^3 + 3.312e04s^2 + 4300s + 185.5 \end{matrix}}$$

and integer order approximate transfer functions of the FOTITO system in Example 2 are

$$G_{11}(s) = \frac{-1.2s^5 - 35.55s^4 + 289.3s^3 + 1744s^2 + 1179s + 107.5}{18.92s^5 + 427s^4 + 2844s^3 + 4836s^2 + 1795s + 109.6}$$

$$G_{12}(s) = \frac{-0.6s^5 - 36.18s^4 + 72.42s^3 + 1154s^2 + 976.3s + 107.7}{81.78s^5 + 1356s^4 + 6712s^3 + 9136s^2 + 3023s + 199.5}$$

$$G_{21}(s) = \frac{-0.5s^5 - 47.95s^4 - 23.64s^3 + 1150s^2 + 1122s + 136.3}{55.5s^5 + 837.9s^4 + 3905s^3 + 6078s^2 + 2858s + 277.5}$$

$$G_{22}(s) = \frac{-1.5s^5 - 64.89s^4 + 173.2s^3 + 1946s^2 + 1493s + 150.2}{46.07s^5 + 811.6s^4 + 4233s^3 + 6098s^2 + 2027s + 120.1}$$

REFERENCES

[1] B. Halvarsson, "Interaction Analysis in Multivariable Control Systems," PhD Thesis, Uppsala University, 2010.

[2] M. A. Üstüner, "Çok Değişkenli Sistemlerde Etkileşimin Yok Edilmesi : Proses Kontrol Sistemi Uygulaması," Master Thesis, Celal Bayar University, 2016.

[3] E. Gagnon, A. Pomerleau, and A. Desbiens, "Simplified, ideal or inverted decoupling?," *ISA Trans.*, vol. 37, no. 4, pp. 265–276, 1998, doi: 10.1016/s0019-0578(98)00023-8.

[4] F. Vázquez and F. Morilla, "Tuning decentralized pid controllers for MIMO systems with decouplers," *IFAC Proc. Vol.*, vol. 15, no. 1, pp. 349–354, 2002, doi: 10.3182/20020721-6-es-1901.00139.

[5] T. Nguyen, L. Vu, and M. Lee, "Design of Extended Simplified Decoupling for Multivariable Processes with Multiple Time Delays," 2011, pp. 1822–1827.

[6] K. Weischedel and T. J. McAvoy, "Feasibility of Decoupling in Conventionally Controlled Distillation Columns," *Ind. Eng. Chem. Fundam.*, vol. 19, no. 4, pp. 379–384, 1980, doi: 10.1021/i100005a026.

[7] C. Rajapandiyan and M. Chidambaram, "Controller design for MIMO processes based on simple decoupled equivalent transfer functions and simplified decoupler," *Ind. Eng. Chem. Res.*, vol. 51, no. 38, pp. 12398–12410, 2012, doi: 10.1021/ie301448c.

[8] M. G. Bulut and F. N. Deniz, "Computation of Stabilizing Decentralized PI Controllers for TITO Systems with Simplified and Inverted Decoupling," *2020 7th Int. Conf. Electr. Electron. Eng. ICEEE 2020*, pp. 294–298, 2020, doi: 10.1109/ICEEE49618.2020.9102547.

[9] M. G. Bulut and F. N. Deniz, "Computation of Stabilizing Decentralized PI Controllers for Fractional Order TITO (FOTITO) Systems," *IEEE 11th Annu. Comput. Commun. Work. Conf. CCWC 2021*, vol. 11, no. 1, pp. 1274–1280, 2021.

[10] L. Liu, S. Tian, D. Xue, T. Zhang, Y. Q. Chen, and S. Zhang, "A Review of Industrial MIMO Decoupling Control," *Int. J. Control. Autom. Syst.*, vol. 17, no. 5, pp. 1246–1254, 2019, doi: 10.1007/s12555-018-0367-4.

[11] A. Numsomran, T. Wongkhum, T. Suksri, P. Nilas, and J. Chaoraingern, "Design of Decoupled Controller for TITO System using Characteristic Ratio Assignment," 2007, vol. 12, no. 3, pp. 957–962.

[12] S. Tavakoli, I. Griffin, and P. J. Fleming, "Tuning of decentralised PI (PID) controllers for TITO processes," pp. 1069–1080, 2006.

[13] G. Kumar, "Control of TITO Process using Internal Model Control Technique," vol. 8, no. 16, pp. 87–92, 2020.

[14] C. Hwang and Y. C. Cheng, "A numerical algorithm for stability testing of fractional delay systems," *Automatica*, vol. 42, no. 5, pp. 825–831, 2006, doi: 10.1016/j.automatica.2006.01.008.

[15] D. Li, X. He, T. Song, and Q. Jin, "Fractional Order IMC Controller Design for Two-input-two-output Fractional Order System," *Int. J. Control. Autom. Syst.*, vol. 17, no. 4, pp. 936–947, 2019, doi: 10.1007/s12555-018-0129-3.

[16] Z. Li and Y. Q. Chen, *Ideal, simplified and inverted decoupling of fractional order TITO processes*, vol. 19, no. 3. IFAC, 2014.

[17] E. O. Mahdouani, M. Ben Hariz, and F. Bouani, "Design of fractional order controllers for TITO systems," *2019 Int. Conf. Signal, Control Commun. SCC 2019*, pp. 179–184, 2019, doi: 10.1109/SCC47175.2019.9116167.

[18] A. San-Millan, D. Feliu-Talegón, V. Feliu-Batlle, and R. Rivas-Perez, "On the modelling and control of a laboratory prototype of a hydraulic canal based on a TITO fractional-order model," *Entropy*, vol. 19, no. 8, 2017, doi: 10.3390/e19080401.

[19] S. Manabe, "Coefficient Diagram Method," *IFAC Proc. Vol.*, vol. 31, no. 21, pp. 211–222, 1998, doi: 10.1016/s1474-6670(17)41080-9.

[20] F. N. Deniz, B. B. Alagoz, N. Tan, and M. Koseoglu, "Revisiting four approximation methods for fractional order transfer function implementations: Stability preservation, time and frequency response matching analyses," *Annu. Rev. Control*, vol. 49, pp. 239–257, 2020, doi: 10.1016/j.arcontrol.2020.03.003.

[21] D. Xue, Y. Chen, and D. P. Atherton, *Linear Feedback Control - Analysis and Design with MATLAB*. Society for Industrial and Applied Mathematics, 2007.

[22] H. Kayan, "Durum Zaman Gecikmeli Sistemler için Kontrol Sistem Tasarımı," Master Thesis, Inonu University, 2014.

[23] M. Yardımcı, "Katsayı Diyagram Yönteminin (KDY) Ölü Zamanlı Sistemlere Uygulanması," Master Thesis, Istanbul Teknik University, 2005.

[24] S. E. Hamamcı, "Zaman Gecikmeli Kararsız Sistemler için Katsayı Diyagram Metodu ile Kontrolör Tasarımı," vol. 6, no. 3, pp. 135–142, 2002.

[25] S. E. Hamamci, "İntegratörlü sistemler için Katsayı Diyagram Metodu ile kontrolör tasarımı," *İTÜ Derg.*, no. 422, pp. 3–12, 2004.

[26] S. Manabe, "Application of Coefficient Diagram Method to Dual-Control-Surface Missile," *IFAC Proc. Vol.*, vol. 34, no. 15, pp. 499–504, 2001, doi: 10.1016/s1474-6670(17)40776-2.

[27] S. Manabe, "Application of coefficient diagram method to MIMO design in aerospace," *IFAC Proc. Vol.*, vol. 15, no. 1, pp. 43–48, 2002, doi: 10.3182/20020721-6-es-1901.01233.

[28] S. E. Hamamci and M. Koksal, "Robust controller design for TITO processes with coefficient diagram method," *IEEE Conf. Control Appl. - Proc.*, vol. 2, no. November, pp. 1431–1436, 2003, doi: 10.1109/cca.2003.1223224.

[29] R. Janani, I. Thirunavukkarasu, and V. S. Bhat, "Experimental implementation of cdm based two mode controller for an interacting 2 * 2 distillation process," *Int. J. Pure Appl. Math.*, vol. 118 (18), no. March, pp. 2241–2251, 2018.

[30] C. Wutthithanyawat and S. Wangnipparnto, "Decentralized PI controller with coefficient diagram method incorporating feedforward controller based on inverted decoupling for two input - Two output system," *Prz. Elektrotechniczny*, vol. 96, no. 9, pp. 159–166, 2020, doi: 10.15199/48.2020.09.33.

[31] C. Wutthithanyawat and S. Wangnippamto, "Design of Decentralized PID Controller with Coefficient Diagram Method Based on Inverted Decoupling for TITO System," *iEECON 2018 - 6th Int. Electr. Eng. Congr.*, vol. 0, pp. 0–3, 2018, doi: 10.1109/IEECON.2018.8712222.

[32] Q. G. Wang, B. Huang, and X. Guo, "Auto-tuning of TITO decoupling controllers from step tests," *ISA Trans.*, vol. 39, no. 4, pp. 407–418, 2000, doi: 10.1016/S0019-0578(00)00028-8.

[33] K. V. T. Waller, "Decoupling in distillation," *AIChE Journal*, vol. 20, no. 3. pp. 592–594, 1974, doi: 10.1002/aic.690200321.

[34] S. Fragoso, J. Garrido, F. Vázquez, and F. Morilla, "Comparative analysis of decoupling control methodologies and H∞ multivariable robust control for variable-speed, variable-pitch wind turbines: Application to a lab-scale wind turbine," *Sustain.*, vol. 9, no. 5, 2017, doi: 10.3390/su9050713.

[35] M. Araki and H. Taguchi, "Two-degree-of-freedom PID controllers,"

Int. J. Control. Autom. Syst., vol. 1, no. 4, pp. 401–411, 2003, doi: 10.11509/isciesci.42.1_18.

[36] N. Tan, A. Yüce, A. Özel, and F. N. Deniz, "Kesirli Dereceli Kontrol Sistemlerinde Tamsayı Dereceli Yaklaşım Metotlarının İncelenmesi," in *Otomatik Kontrol Ulusal Toplantısı, TOK'14*, 2014, pp. 556–561.

[37] A. Oustaloup, F. Levron, B. Mathieu, and F. M. Nanot, "Frequency-band complex noninteger differentiator: Characterization and synthesis," *IEEE Trans. Circuits Syst. I Fundam. Theory Appl.*, vol. 47, no. 1, pp. 25–39, 2000, doi: 10.1109/81.817385.

[38] K. Matsuda and H. Fujii, "H∞ optimized wave-absorbing control: Analytical and experimental results," *J. Guid. Control. Dyn.*, vol. 16, no. 6, pp. 1146–1153, 1993, doi: 10.2514/3.21139.

[39] F. N. Deniz, B. B. Alagoz, N. Tan, and D. P. Atherton, "An integer order approximation method based on stability boundary locus for fractional order derivative/integrator operators," *ISA Trans.*, vol. 62, pp. 154–163, 2016, doi: 10.1016/j.isatra.2016.01.020.

[40] F. N. Deniz, "Kesir Dereceli Sistemlerde Modelleme ve Kontrol Uygulamaları," PhD Thesis, Inonu University, 2017.

[41] "Integer order approximation for fractional order derivative - File Exchange - MATLAB Central." [Online]. Available: https://nl.mathworks.com/matlabcentral/fileexchange/87357-integer-order-approximation-for-fractional-order-derivative?s_tid=srchtitle." .

BIOGRAPHIES

MİRAY GÜNAY BULUT received the B.S. degree in electrical and electronics engineering from Meliksah University, in 2016. She received the M.S in electrical and electronics engineering from Inonu University Malatya, Turkey in 2021. Her research interests are control systems applications.

FURKAN NUR DENİZ graduated from Inonu University department of Electrical and Electronics Engineering in 2008. She received her Ph.D. degree in Electrical and Electronics Engineering from Inonu University in 2017. Her research interests include fractional order control systems, modeling, and simulation.